4.2.3.4 Dynamics and thermal evolution

DORIS BREUER

4.2.3.4.1 Introduction

4.2.3.4.1.1 Symbols used

Symbol	Definition
a	Constant parameter of *Nu*-*Ra* relation (definition of *Nu* and *Ra*, see below)
α	Thermal expansivity
A_m	Surface area of the mantle
A_c	Surface area of the core
b	Depth of the convecting mantle
β	First exponent of *Nu*-*Ra* relation (definition of *Nu* and *Ra*, see below)
c	Second exponent of Nu-*Ra* relation (definition of *Nu* and *Ra*, see below)
C_p	Specific heat at constant pressure
C_m	Specific heat of the mantle
C_c	Specific heat of the core
δ_{cm}	Thickness of the lower thermal boundary layer
δ_{ij}	Kronecker delta
ΔT	Temperature difference across the convecting mantle
ΔT_r	Characteristic temperature difference
ΔT_{cm}	Temperature difference across the lower thermal boundary layer
E	Activation energy for creep
ε_m	Ratio between the mantle temperature that is representative of the internal energy of the mantle and T_m (definition of T_m, see below)
ε_c	Ratio between the mantle temperature that is representative of the internal energy of the core and T_{cm} (definition of T_{cm}, see below)
f	Constant for the Frank-Kamenetskii approximation
Φ	Dissipation function
g_i	Acceleration of gravity
h	Grain size
H	Rate of internal heat production per unit mass
H_m	Rate of mantle heat production per unit mass
η	Dynamic viscosity
k	Thermal conductivity
κ	Thermal diffusivity
λ	Decay constant
n	Stress component
Nu	Nusselt number
p	Pressure
q_s	Surface heat flow
q_m	Heat flow out of the mantle
q_c	Heat flow out of the core into the mantle
R	Universal gas constant
Ra_H	Internal heating Rayleigh number
Ra	Rayleigh number
Ra_i	Rayleigh number based on the viscosity at the base of the upper thermal boundary layer
Ra_δ	Lower thermal bounadyr layer Rayleigh number
ρ	Density
ρ_m	Density of the mantle
ρ_c	Density of the core
t	Time
T	Temperature
T_m	Temperature of the isothermal mantle below the conductive layer

T_{cm}	Temperature at the core-mantle boundary
τ	Second invariant of the deviatoric stress tensor
τ_{ij}	Deviatoric stress tensor
u_i	Fluid velocity
V	Activation volume
V_m	Volume of the mantle
V_c	Volume of the core
x_i	Position vector

4.2.3.4.1.2 Overview

The thermo-chemical evolution of terrestrial planets depends on their composition, structure, rate of internal heat production, and, to a large extent, on the dynamics of the planet's mantle through which heat is transported by thermal and chemical convection. An understanding of the thermo-chemical evolution is essential for any interpretation of surface features as being caused by the interior dynamics. The Earth with plate tectonics and life is unique among the terrestrial planets. Earth's lithosphere (the outer rigid layer of the planet) is broken in seven major plates that participate in the mantle convection cycle. At mid-oceanic ridges rock is added to the plates while at subduction zones plates are subducted. Heat transfer across the Earth's surface is mostly by advection at mid-oceanic ridges but conduction through the plates away from the ridge also contributes as does volcanism that is not related to plate margins (e.g., the Hawaian chain volcanoes). The mode of convection that is related to plate tectonics is termed mobile lid convection. The near-surface lithospheres of the other earth-like planets are not segmented but consist of single plates, so called stagnant lids, beneath which the mantle convects. Heat flow through the lithosphere is mainly transported by conduction, with some minor contribution by volcanic heat transport through this stagnant lid. The difference in the heat transport mechanism for the planets is also reflected in their thermal evolution. In the following section, we will introduce the basic equations for convection and thermal evolution calculations and describe fundamental differences in the main convecting regimes, between stagnant lid regime and mobile lid convection. In the last part, we summarize important aspect of the thermo-chemical evolution of Mercury, Venus, Mars and the Moon.

4.2.3.4.2 Thermal and chemical convection

The dynamics of the interior of terrestrial planets is mainly driven by thermal convection. When the mantle is heated from within (or from below) and is cooled from above, it may become gravitationally unstable and thermal convection can occur as colder rock descends into the mantle and hotter rock ascends toward the surface. The stability of the mantle is mostly determined by a balance between the thermal buoyancy and the retarding viscous forces and is measured by the dimensionless Rayleigh number *Ra* (compare Table 1). Convection transports heat toward the surface of the planet and tends to cool the interior, while heat produced within, e.g., by the decay of radioactive elements tends to warm it. The motions driven by convective heat transport result in surface stresses and deformation, producing the geologic features observed on the terrestrial bodies today. The planet's internal heat sources provide the energy for its dynamics, supplying it with the driving energy for mantle convection, and for melting the mantle which may lead to volcanism. The internal energy of the terrestrial planets was greater early in their histories than it is today, having accumulated rapidly by heat conversion associated with three separate processes, all of which were most intense during the first few million years of the planet's history: (1) accretion of the planet by impacts, (2) core formation and the associated release of gravitational potential energy, and (3) the radioactive decay of unstable isotopes. Another important heat source in a terrestrial body can be tidal dissipation as in the case of the Galilean satellites. This heat source is not necessarily higher early in the evolution; rather, it depends on the body's orbital and thermal evolution.

Purely thermal convection can be strongly influenced by chemical layering in the mantle. In the case of chemical layering, density variations that drive convection may not only be caused by temperature variations but also by variations in chemical composition. Chemical layering may even block or retard thermally driven mantle flow if the density increases with depth. In this case, thermal convection is only possible if density changes due to temperature variations can overcome the compositional density differences. Chemical layering can enhance mantle flow if the density decreases with depth. Reshuffling of this unstable configuration results in a stable density configuration unless efficient mixing prevents the establishment of distinct layers. It is also possible that thermal convection takes place in separate and chemically distinct layers. The heat transport in a mantle with layered thermal convection is less efficient than in a mantle with whole mantle convection. Chemical stratification resulting from early differentiation of the mantle is one way to explain the presence of separate and chemically distinct reservoirs that might be needed to explain geochemical observations. At present, we do not know whether distinct chemical reservoirs exist in the terrestrial planets.

4.2.3.4.3 Field equations and parameterization

4.2.3.4.3.1 Field equations

To describe flow processes in a planetary mantle we must consider the conservation of mass, momentum, and energy for a fluid continuum, since the solid rocks of a mantle deform as fluids on geological time scales. In addition, these conservation equations must be supplemented by an equation of state. In the following the basic equations are listed. More details can be found e.g. in [01Sch].
The conservation of mass:

$$\frac{1}{\rho}\frac{D\rho}{Dt} + \frac{\partial u_i}{\partial x_i} = 0 \tag{1}$$

The conservation of momentum (Navier-Stokes-Equation):

$$\rho\frac{Du_i}{Dt} = -\frac{\partial p}{\partial x_i} + \frac{\partial}{\partial x_j}\left[\eta\left(\frac{\partial u_i}{\partial x_j} + \frac{\partial u_j}{\partial x_i} - \frac{2}{3}\delta_{ij}\frac{\partial u_k}{\partial x_k}\right)\right] + \rho g_i \tag{2}$$

The conservation of energy:

$$\rho c_p \frac{DT}{Dt} - \alpha T\frac{Dp}{Dt} = \frac{\partial}{\partial x_i}\left(k\frac{\partial T}{\partial x_i}\right) + \Phi + \rho H \tag{3}$$

with $\frac{D}{Dt} = \frac{\partial}{\partial t} + u_i\frac{\partial}{\partial x_i}$ and the dissipation function Φ is defined as

$$\Phi = \tau_{ij}\frac{\partial u_i}{\partial x_j} \tag{4}$$

These general equations can be simplified by assuming a linearized equation of state for the mantle density of the form:

$$\rho = \bar{\rho}(\bar{T}, \bar{p}) + \rho' \tag{5}$$

where the overbars refer to a reference state and the prime to departure from the reference state :

$$T = \bar{T} + T', \quad p = \bar{p} + p' \tag{6}$$

It is convenient to take the reference state as motionless and steady. The equations are non-dimensionalized to obtain the following dimensionless variables (denoted with an asterix)

$$T'^* = \frac{T'}{\Delta T_r} \tag{7}$$

$$\rho^* = \frac{\rho}{\rho_r} \tag{8}$$

$$p'^* = \frac{p' b^2 \rho_r c_{pr}}{\eta_r k_r} \tag{9}$$

$$u_i^* = \frac{u_i b \rho_r c_{pr}}{k_r} \tag{10}$$

$$x_i^* = \frac{x_i}{b} \tag{11}$$

$$t^* = \frac{t k_r}{b^2 \rho_r c_{pr}} \tag{12}$$

where the subscript r refers to a representative parameter value. With the help of the dimensionless variables simplifying approximations such as the anelastic or Boussinesq approximation can be easily introduced.

Table 1. Important dimensionless parameters used for fluid dynamics field equations.

Symbol	Dimensionless parameters	
Pr	Prandtl number	$\mathrm{Pr} = \frac{\mu_r c_{pr}}{k_r}$
Ra	Rayleigh number	$Ra = \frac{\alpha_r \rho_r g_r \Delta T_r b^3}{\eta_r \chi_r}$
Ra_H	Internal heating Rayleigh number	$Ra_H = \frac{\alpha_r \rho_r^2 g_r H_r b^5}{\eta_r \chi_r k_r}$
D	Dissipation number	$D = \frac{\alpha_r g_r b}{c_{pr}}$
Nu	Nusselt number	$Nu = \frac{qb}{k\Delta T}$

For both approximations, the inertial forces in the momentum equation are neglected because the Prandtl number is essentially infinite. The anelastic approximation further ignores the partial derivatives of density with respect to time in the momentum equation and thereby eliminates fast local density variations, i.e. seismic waves. The Boussinesq approximation, leading to the simplest form of the system of equations, takes all thermodynamic variables including the density to be constant, but a buoyancy force due to temperature variations is included in the vertical force balance equation. The equations (1) to (3) then reduce to:

$$\frac{\partial u_i^*}{\partial x_i^*} = 0 \tag{13}$$

$$0 = -\frac{\partial p_i'^*}{\partial x_i^*} - \overline{g}_i^* T'^* Ra + \frac{\partial}{\partial x_j^*}\left\{\eta^*\left(\frac{\partial u_i^*}{\partial x_j^*} + \frac{\partial u_j^*}{\partial x_i^*}\right)\right\} \tag{14}$$

$$\overline{\rho}^* \overline{c}_p^* \frac{DT'^*}{Dt^*} = \frac{\partial}{\partial x_i^*}\left(\overline{k}_i^* \frac{\partial T'^*}{\partial x_i^*}\right) + \overline{\rho}^* H^* \frac{Ra_H}{Ra} \tag{15}$$

4.2.3.4.3.2 Parameterized convection

Because of the inherent complexity in these models it is often desirable to take an empirical approach and parameterize the convective heat transfer rate as a function of known quantities. Such parameterizations can be derived using simple theories, which result in scaling laws that describe the heat transport in the interior as a function of the convective parameters. Our improving understanding of the heat transport mechanisms on terrestrial planets over the last two decades has led to repeated changes in the preferred scaling law used to model the thermal evolution of one-plate planets. Initially, the scaling law for a fluid with constant viscosity was used for one-plate planets [e.g., 83Ste, 88Sch, 92Sch]. Today, the stagnant-lid model allows the variations of viscosity with temperature to be incorporated.

From convection experiments and boundary layer theory for isoviscous fluids the classical power law relationship between heat flow and convective parameters [e.g., 67Tur, 79Rob] has been derived:

$$Nu = a \cdot Ra^{\beta} \tag{16}$$

This equation relates the dimensionless heat flux out of the convecting layer, expressed as the Nusselt number, Nu, to the strength of thermal convection as measured by the Rayleigh number, Ra.

Table 2. The fitting coefficients to calculate the scaling law for isoviscous convection (eq. 18). F/F: top and bottom boundaries are free slip; F/R: top is free slip and bottom is rigid; R/F: top is rigid and bottom is free slip; R/R: top and bottom boundaries are rigid.

a	β	Boundary conditions	References
0.294	0.333	F/F	67Tur
0.279	0.313	F/F	82Jar
0.2697	0.3185	F/F	84Chr
0.268	0.319	F/F	85Sch
0.250	0.323	F/F	93Han
0.195	0.3	F/R	79Kve
0.332	0.225	R/R	83Fri
0.258	0.321	F/F	00Des
0.336	0.252	R/F	00Des
0.339	0.223	R/R	00Des

In the meantime, it has been recognized that this scaling law models the heat transport in a planet where convection comprises the whole mantle including the outer layers. In fact, such a model describes the heat transport in a planet with plate tectonics better than that in a one-plate planet [01Sch]. For a strongly temperature dependent viscosity convection occurs in the stagnant lid regime as suggested for the terrestrial planets apart from the Earth. The most viscous part of the lithosphere is essentially rigid and convection involves only a thin layer of the bottom of the lithosphere. The scaling law for stagnant lid convection, thus, depends also on the mantle viscosity according to

$$Nu = a\Theta^{-c} Ra_i^{\beta} \tag{17}$$

with Ra_i the Rayleigh number based on the viscosity at the base of the upper thermal boundary layer and the Frank-Kamenetskii parameter

$$\Theta = \frac{E}{RT_m^2} \Delta T \tag{18}$$

The heat flow out of the convecting system, i.e., the mantle heat flow, is given by

$$q_m = Nu \frac{k \Delta T}{b} \tag{19}$$

The heat flow into the convecting system, i.e., the core-mantle heat flow, can be calculated by a local stability criterion [e.g., 83Ste, 00Des]

$$q_c = \frac{k\Delta T_{cm}}{\delta_{cm}} \tag{20}$$

with

$$\delta_{cm} = \left(\frac{\eta \kappa Ra_\delta}{\alpha \rho g \Delta T_{cm}} \right)^{1/3} \tag{21}$$

The lower thermal boundary layer Rayleigh number has been identified to depend on Ra_i [00Des], unlike the case for an isovisous fluid

$$Ra_\delta = 0.28 Ra_i^{021} \tag{22}$$

The constant parameters to calculate Nu depend on the stress component, the heating mode and the geometry. Values of various numerical models are given in Table 3. Note that q_c is zero for internal heating modes.

Table 3. Parameter values for scaling laws for stagnant lid convection (Eq. 17) derived by fitting the results of numerical simulations. There is a change in the scaling relationship from steady state convection to time-dependent convection at a Rayleigh number of about 10^6 [99Dum].

a	c	β	Heating mode	Geometry	References
		n = 1, steady state			
1.89	1.02	0.2	Bottom heating	1 × 1	95Mor, 96Sol
1.99	1.0	0.2	Bottom heating	1 × 1	99Dum
3.8	1.63	0.258	Bottom heating	1 × 1	00Des
2.51	1.2	0.2	Internal heating	Spherical	99Res
		n = 1, time dependent			
0.54	1.333	0.333	Bottom heating	4 × 1	97Doi
0.52	1.333	0.333	Bottom heating	4 × 1	99Dum
0.53	1.333	0.333	Internal heating	4 × 1	00Sol
0.57	1.333	0.333	Internal heating	2 × 1	98Gra
0.67	1.333	0.333	Internal heating	Spherical	05Res
		n = 3, steady state			
2.8	0.96	0.29	Bottom heating	1 × 1	98Res
2.1	1.33	0.33	Bottom heating	4 × 1	99Dum
		n = 3, time dependent			
0.87	1.6	0.6	Bottom heating	4 × 1	99Dum
0.97	1.6	0.6	Internal heating	1 × 1	99Res, 00Sol

To calculate thermal evolution models for terrestrial planets using the parameterizations, energy balance equations for the mantle and the core need to be solved. These are, respectively:

$$\rho_m C_m V_m \varepsilon_m \frac{dT_m}{dt} = -q_m A_m + \rho_m H_m V_m , \tag{23}$$

$$\rho_c C_c V_c \varepsilon_c \frac{dT_{cm}}{dt} = -q_c A_c . \tag{24}$$

Detailed discussions of these equations and the methods used to derive them can be found in the literature. Some of these models include the growth of a crust by mantle partial melting and differentiation and the associated redistribution of radioactive elements and convection in the core generation as a prerequisite for the generation of magnetic fields [83Ste, 02Hau, 04Hau, 03Bre, 06Bre].

4.2.3.4.4 Material parameters: viscosity and radioactive heat sources

4.2.3.4.4.1 Mantle rheology and viscosity

The exponential dependence of the viscosity on the inverse absolute temperature is the most important parameter for understanding the role of mantle convection in transporting heat. The temperature dependence of the viscosity acts as a thermostat to regulate the mantle temperature. In addition to the temperature dependence, the rheology in a planetary mantle can be described by two main creep mechanisms: diffusion creep and dislocation creep. For the case of diffusion creep the solid behaves as a Newtonian fluid where the viscosity is independent of the applied shear stresses. In contrast, for dislocation creep, the solid behaves as a non-Newtonian fluid where viscosity depends on shear stress. Indeed, viscosity tends to decrease with increasing shear stress, often nonlinearly. Which creep mechanism is valid in terrestrial mantles is not certain. Most laboratory studies of mantle deformation have concluded that dislocation creep is the applicable deformation mechanism in the upper Earth mantle and diffusion creep in the lower mantle [01Sch]. However, this assumption is not consistent with post-glacial rebound studies that favor diffusion creep also for the upper mantle. Furthermore, laboratory measurements have shown that the pressure-dependence on viscosity can not be neglected in a terrestrial mantle [97 Kar]. Thus, the viscosity of a terrestrial mantle can be described with the following Arrhenius relationship:

$$\eta = \frac{\mu^n}{2A}\left(\frac{1}{\tau}\right)^{n-1}\left(\frac{h}{B^*}\right)^m \exp\left(\frac{E+pV}{RT_m}\right) \tag{25}$$

with B^* the length of the Burgers vector (~0.5 nm) and μ the shear moduls (~80 GPa). For a Newtonian rheology n is equal to 1 and for a non-Newtonian rheology a typical value of n is 3.5. For most numerical studies, however, an exponential viscosity, i.e., the Frank-Kamenetskii approximation, is used since the two give almost identical results in the limits of large viscosity contrasts.

$$\eta = \frac{f}{\tau^{n-1}}\exp(-\gamma T) \tag{26}$$

where f is a constant and γ is related to equation (26) through $\gamma = E/RT_i^2$ for purely temperature-dependent viscosity. In the case of large viscosity variations due to significant temperature variations in a terrestrial mantle both equations (25) and (26) give similar results in terms of the viscosity in the convecting part of the mantle and the flow characteristic.

Table 4. Flow law parameters for olivine. Dry refers to water-free and wet to water-saturated conditions, respectively.

	Dislocation creep		Diffusion creep	
	Dry	Wet	Dry	Wet
A [s^{-1}]	3.5×10^{22}	2.0×10^{18}	8.7×10^{15}	5.3×10^{15}
n	3.5	3.0	1.0	1.0
m	0	0	2.5	2.5
E [kJ mol^{-1}]	540	430	300	240
V [cm^3 mol^{-1}]	10-25	10-20	6	5
h [m]	-	-	10^{-2} - 1	10^{-2} - 1

4.2.3.4.4.2 Radioactive heat sources

The most important heat source in a planetary body – after planetary accretion and core formation – is the release of energy by the decay of long-lived radioactive elements. These elements, namely the uranium isotopes ^{235}U and ^{238}U, the thorium isotope ^{232}Th, and the potassium isotope ^{40}K, are distributed into the mantle and the crust. The total present-day production H_0 is related to the heat generation rates of the individual radioactive elements by

$$H_0 = C_0^U \left(H^U + \frac{C_0^{Th}}{C_0^U} H^{Th} + \frac{C_0^K}{C_0^U} H^K \right) \tag{27}$$

and the past mean heat production rate is given by

$$\begin{aligned} H = {} & 0.9928 C_0^U H^{U^{238}} \exp\left(\frac{t \ln 2}{\tau_{1/2}^{U8}} \right) \\ & + 0.0071 C_0^U H^{U^{235}} \exp\left(\frac{t \ln 2}{\tau_{1/2}^{U^{235}}} \right) \\ & + C_0^{Th} H^{Th} \exp\left(\frac{t \ln 2}{\tau_{1/2}^{Th}} \right) \\ & + 1.19 \cdot 10^{-4} C_0^K H^{K^{40}} \exp\left(\frac{t \ln 2}{\tau_{1/2}^{K^{40}}} \right) \end{aligned} \tag{28}$$

The rates of heat production and the half lives $\tau_{1/2}$ of these isotopes are given in Table 5 and values of the concentration of the isotopes for various terrestrial bodies are listed in Table 6.

Table 5. Radiogenic heat sources in terrestrial planets.

Isotope	Specific heat production rate H [W kg^{-1}]	Half life of the isotope $\tau_{1/2}$ [a]
^{238}U	9.46×10^{-5}	4.47×10^{9}
^{235}U	5.69×10^{-4}	7.04×10^{8}
U	9.81×10^{-5}	
^{232}Th	2.64×10^{-5}	1.40×10^{10}
^{40}K	2.92×10^{-5}	1.25×10^{9}
K	3.48×10^{-9}	

4.2.3.4.5 Dynamics and thermal evolution of terrestrial planets

The thermal evolution of a terrestrial planet depends on the state of its outer lid and differs between models that have a stagnant lid and those that have a mobile lid or plate tectonics. A comparison of the two regimes while assuming the same parameter values for a generic planet similar to Mars shows substantial differences. For the stagnant lid planet the lid will thicken rapidly as the planet cools while the temperature of the underlying convecting mantle and core will change comparatively little (Figs. 1a and 1b). With plate tectonics, there is, of course, no growth of a lid and the cooling of the deep interior is more efficient. As a typical feature, the stagnant lid grows rapidly during the first few hundred million years and the growth slows down considerably thereafter.

Figures 1c and 1d compare the cumulative energy loss, i.e., the energy loss over the entire evolution of the planet, and the surface heat flow of the two models. After 4.5 Ga, the energy loss is about 3.1×10^{29} J smaller for the stagnant lid model as compared to the plate tectonic model. Such energy losses, when distributed homogeneously over the entire mantle, imply that the present-day mantle is about 600 K cooler in the plate tectonics model than it is in the stagnant lid model. Interesting to note is that variations in the initial temperature distribution results in similar results for the present-day values of the temperature, surface heat flow, and stagnant lid thickness for both regimes (seen Fig. 1). Any tendency of the mean temperature to increase is offset by an associated reduction in mantle viscosity, an increase in convective vigor, and a more efficient outward transport of heat. Similarly, a decrease in mantle temperature tends to increase mantle viscosity, reduce convective flow velocities, and decrease the rate of heat transfer. As a result of the sensitive feedback between mantle temperature and rheology, relatively small changes in temperature can produce large changes in heat flux, and the temperature is consequently buffered at nearly constant temperature [65Toz].

The rate at which a planet loses its internal heat to space, i.e., the surface heat flow, is an important parameter describing the internal activity of a planet. It further controls the level of tectonism (faulting and folding of the planet's surface due to internal deformation) and volcanic activity on the planet. It may be speculated that a planet, in which heat is transported effectively by plate tectonics, has a higher surface heat flow than a planet in the stagnant lid regime. However, this is only true in the early evolution. In the shown example, the surface heat flow is even slightly higher in the stagnant lid model after about 2.5 Ga. The contribution of secular cooling at present is, therefore, similar for the convecting regimes assuming the same mantle parameters. The Urey ratio, i.e., the ratio of the heat produced within the mantle by radioactive decay to the total surface heat flow has present values of 0.6 for the stagnant lid regime and 0.7 with plate tectonics. A detailed description of the differences between the regimes can be found in [07Bre].

Table 6. Models for the present-day concentration of radioactive elements in the primitive mantle of the planets (for comparison C1-chondrites are included in the table). H_0 is the heat production rate per mass 4.5 Ga ago and H_p is the present-day heat production rate per mass. The models for the Moon indicated with * give values for the primitive mantle plus the core. As the core size is assumed to be very small the difference to models only considering the abundances in the silicate part only is small.

Planet	Concentration			H_0	H_p	Reference
	U [ppb]	Th [ppb]	K [ppm]	[pW/kg]	[pW/kg]	
Mercury	30	120	0	19	5.9	78Wei
	8	30	550	24	3.4	88Cam, 88Wet
	0	400	0	13	10	87Feg
Venus	22	79	220	23	5	80Mor
Mars	16	64	160	17	3.7	86Tre
	28	101	62	21	5.0	79Mor
	16	56	305	23	4.	94Wae
	16	55	920	49	6.1	97Lod
Earth	20.3	79.5	240	23	5	95Mcd
	22	78.2	232.4	22	5	93Kar
	21	84.1	240	23.5	5.1	91Rin
	18	64	180	19	4	85Tay
Moon	60.9	223	178	47	12.5	77Wae
	33	125	83	25	6.8	82Tay*
	62.8	224	102	45	15	77And*
C1-Chondrites	7.4	29	550	24	3.4	95Mcd

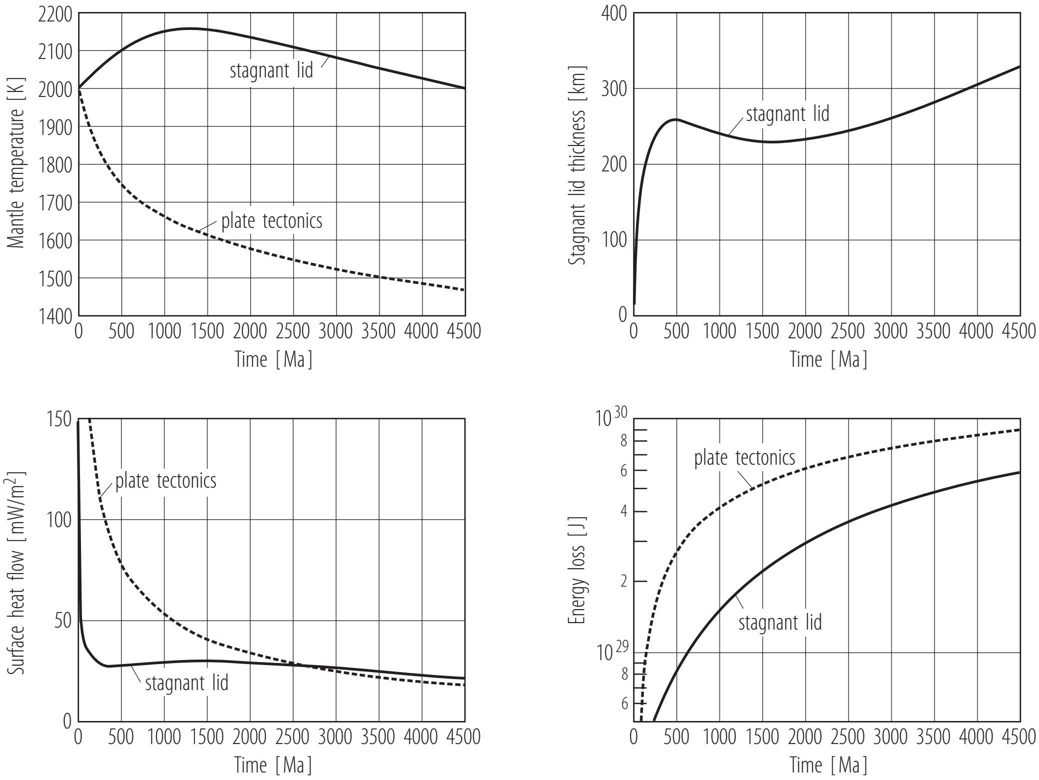

Fig. 1. Mantle temperature, stagnant lid thickness, surface heat flow and energy loss for two different heat transfer models: stagnant lid convection (solid line) and plate tectonics (dashed line). The models shown are for parameters representative of Mars.

Table 7 Rayleigh number and surface heat flow values representative of the present internal activity of the terrestrial planets. Variations in the Rayleigh number are mainly due to the uncertainties in the mantle viscosity, whereas variations in the surface heat flow are mainly due to uncertainties in the radioactive heat source content of the primitive mantle (compare Table 6) and the contribution of secular cooling (values between 20% and 50% have been assumed). The surface heat flow of the Earth is based on thermal gradients in boreholes and corrected for the observational underestimation due to hydrothermal circulation [93Pol, 07Jau]. The contribution of secular cooling is about 50%. In the case of Mercury the Rayleigh number can be below the critical Rayleigh number of convection; thus, a present conductive mantle is possible. The surface heat flow of the Moon has been also measured at two different places; these values are at the lower end of the values given here (compare Table 8).

	Rayleigh number	Surface heat flow [mW/m^2]
Mercury	conductive - 10^5	9 - 30
Venus	10^7 - 10^8	54 - 88
Mars	10^6 - 10^7	15 - 30
Earth	10^7 - 10^8	82 - 90
Moon	10^5 - 10^6	16 - 38

In the following, we list important characteristics of the thermo-chemical evolution of Mercury, Venus, Mars and the Moon. More detailed discussions can be found in the indicated literature.

4.2.3.4.5.1 Mercury

An important constraint on Mercury's thermal evolution are lobate scarps that are more or less evenly distributed over the well-imaged portion of the surface. The scarps are thought to indicate an average contraction of the planet's radius by only 1 - 2 km since the end of heavy bombardment [75Str]. The most likely source of global contraction is a combination of a thermal contraction (reduction in average internal temperature) and a phase change by solidification (e.g., growth of an inner core). Core freezing contributes more to the global contraction [76Sol].

Thermal evolution models [88Sch, 04Hau] indicate that the observed scarps account for only a rather small fraction of the total contraction. One possible explanation is that much of the contraction would have predated the observable geologic record, for instance most of the inner core was formed before the end of heavy bombardment. In any case, to meet the constraint of only 1 - 2 km of contraction since the end of heavy bombardment, relatively little cooling of the interior should have happened since that time. Of the three formation models [78Wei, 88Cam, 88Wet, 87Feg], the vaporization model [87Feg] predicts less cooling and contraction of the planet [04Hau] as it assumes ^{232}Th as the sole radiogenic heat producing element of relevance, which with its 14 Gyr half-life has not had a significant decline in heat output.

The question of whether mantle heat transport in Mercury occurs by conduction or convection is controversially discussed in the literature and depends mainly on assumptions about the initial thermal state, the amount and distribution of radioactive elements, and the efficiency of heat transport. Early models that assume an undifferentiated and thus respectively cold Mercury suggest that the planet cools conductively throughout its evolution [e.g., 74Sie, 76Sha, 76Sol, 77Sol, 79Sol]. Models that assume an initially hot and fully differentiated Mercury are in favour of convection [76Sol, 79Toz, 83Ste, 88Sch, 99Con]. The results suggest that thermal convection is likely during the entire evolution of the planet although it can be very sluggish at present. Recent studies [01Sol, 04Hau] that consider a non-Newtonian rheology and incorporate crust growth have a convecting mantle only during the early stages of evolution which is accompanied by extensive melting and differentiation. Later, convection and melting are absent and the planet cools conductively.

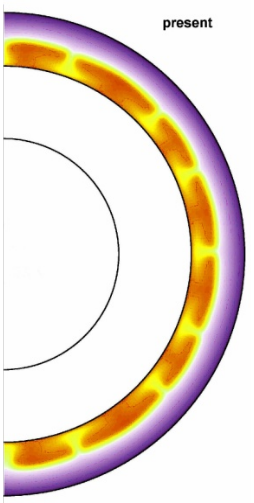

Fig 2. (see also color-picture part, page 620) A typical temperature field of the convecting mantle (coloured region) in Mercury calculated with a 2D axisymmeteric convection model with strongly temperature and pressure dependent viscosity. The temperature decreases from brownish colours to yellow, violet, and blue. The upper violet to blue part is the stagnant lid, convection takes place underneath. The solid circle in the center indicates the present size of the inner core. The viscosity increases by a factor of 10 in the convecting mantle and by 5 orders of magnitude in this model of the lid. The model assumes a concentration of radioactive heat sources consistent with the silicate vaporization model [87Feg] and a concentration of 1 wight-% sulfur in the core [after 99Con].

The observed magnetic field of the planet implies the presence of a fluid outer core. To prevent the core from freezing completely, radioactive heat sources in the core [78Tok], late core formation [76Sha, 77Sol] and deep mantle heat sources [76Cas] have been suggested. Late core formation would support a cool initial state for Mercury but is at variance with accretion models [e.g., 88Sch]. The most likely reason for Mercury not having a totally frozen core, however, is a small but significant concentration of a light alloying element in its core that would reduce the core melting temperature. Sulfur is the most likely candidate [77Rin, 83Mcc] as it is cosmochemically easily available and siderophile. To satisfy the observations of both a planet-wide contraction of a few kilometers and a present fluid outer core, thermal evolution studies [88Sch, 99Con, 04Hau, 06Bus, 07Bre2] conclude that the mantle should be dry and strongly depleted in potassium.

4.2.3.4.5.2 Venus

The surface of Venus has a global average age of 300 to 800 Ma [92Sch, 97Mck]. It has been suggested [97Mck, 97Bou, 98Nim] that the planet was globally resurfaced by a volcanic event about 700 Ma b.p.. The resurfacing event – according to these models – was followed by an epoch of volcanic quiescence lasting to the present day. The cause for this global resurfacing event and whether it was a single event or one of a periodically recurring set of events is highly uncertain. However, the reality of a rapid global resurfacing event has been questioned by [99Cam] and most recently by [06Bon]. According to the latter authors, the cratering record allows a variety of interpretations in terms of volcanic resurfacing including a global decrease with time in the rate of an otherwise statistically distributed volcanic activity. Previous authors had concluded that Venus underwent a major transition in tectonic style albeit more gradual than the previously postulated sudden global resurfacing event. The surface geology also seems to indicate that modifications of the surface are planet wide and gradual over long periods of time rather than episodic and locally confined [06Iva].

The lack of a present dynamo does not imply that Venus never had an intrinsic magnetic field although we have no information that relates directly to the past history of the field. Thermal evolution models suggest that there was a magnetic moment of Venus of the same order as Earth's for about the first three billion years of Venus' history [83Ste]. An alternative scenario for the present lack of a Venus magnetic field suggests that Venus's field ceased as Venus transitioned from a plate tectonic to a stagnant lid regime around 700 Ma ago [02Ste].

4.2.3.4.5.3 Mars

A fundamental problem in the evolution of Mars is the timing and the origin of the crustal dichotomy. The southern highlands and northern lowlands of Mars differ markedly in average elevation [99Smi] and crustal thickness [00Zub, 04Neu]. Although it is generally accepted that this crustal dichotomy is one of oldest features on Mars, the exact timing of the dichotomy formation, which has implications for the formation mechanism, is strongly debated. The time of formation varies between the Late Noachian/Early Hesperian (3.7 Ga) [90Mcg], the Early Noachian or earlier (>3.9 Ga) [02Fre, 05Nim], and even as early as the first 50 Ma after the solar system formation [05Sol]. The origin of the crustal dichotomy has variously been related to external processes, i.e. one or several impacts [84Wil, 88Fre,08And, 08Nim, 08Mar] and internal processes [e.g., 79Wis], but none of the proposed formation mechanisms has been fully convincing in part due to the uncertainty in the timing of the dichotomy formation. For an endogenic origin of the dichotomy, three different mechanisms have been proposed that are associated with 1) the evolution of an early magma ocean [01Hes, 05Elk], 2) an episode of degree-one mantle convection [73Sch, 79Wis, 01Zho], and 3) an early phase of plate tectonics [94Sle].

The proposed scenarios for the formation of the crustal dichotomy have differing implications for the thermal evolution of Mars, in particular, for the early evolution. At the present time and most likely during the past 4 Ga, Mars has been in the stagnant lid regime with a stable plate overlying the convecting mantle. For the first few hundred million years, however, little is known with any certainty, in particular, whether the planet had a phase of plate tectonics and later transitioned to single-plate tectonics or whether the planet never changed its heat transport mechanism and always was in the stagnant lid regime.

[94Sle] proposed that the smooth northern lowlands and the Tharsis volcanoes were remnants of an ocean floor and an island arc volcanic chain, respectively, similar to plate tectonic features on Earth. More recently, the magnetic lineation patterns on parts of the southern highlands detected by Mars Global Surveyor (MGS) have been interpreted to be the result of plate divergence [99Con2, 05Con]. The dating of the magnetic anomalies led the authors to suggest that the potential early plate tectonic regime lasted about 500 Ma. However, there is no finally convincing geological evidence for the early existence of plate tectonics on Mars.

Another striking surface feature are the large volcanic provinces, Tharsis and Elysium, where the volcanic activity lasted for billion years until the recent past [99Har, 02Ber, 04Neu]. The persistence of volcanism in Tharsis and Elysium could be explained by invoking longstanding plumes with substantially higher temperature (i.e., more than 100 K) than the average mantle. Such a plume must be thermally fed by energy flowing from a hot core. As causes for the stability of the super plumes deep-mantle phase transitions [95Wei, 96Har, 98Bre, 00Har], chemical layering in the mantle, variations in mantle thermal conductivity [01Sch], and the crustal dichotomy [04Wen] have been proposed. Most recently, thermal blanketing of the mantle by a thickened crust [06Sch, 07Sch] has been discussed as an alternative mechanism for generating melt underneath these volcanic provinces. This mechanism would not require a super-plume and may be more consistent with a cooling core [01Spo].

Thermo-chemical evolution models that include crustal growth usually predict that most of the crust formed during the first billion years and has grown to reach a thickness of tens of kilometers [91Spo, 92Sch, 93Bre, 02Hau, 03Bre, 06Bre, 07Sch] to a few hundred kilometers [01Wei]. The results of the model calculations are consistent with the observation that most of the crust was produced early on [05Sol, 05Nim].

At present, Mars has no global dipolar magnetic field, but the presence of a strong magnetization of the oldest parts of the crust [98Acu, 99Acu, 99Con2, 01Acu] suggests that the planet generated a magnetic field early in its history. An early dynamo is supported by most thermal evolution models that consider the magnetic field history [e.g., 90Sch, 98Spo, 02Hau, 03Bre, 06Bre, 04Wil]. The models arrive at an early thermally driven dynamo as a consequence of rapid cooling of a core initially superheated with respect to the mantle (Fig. 3). An alternative scenario assumes rapid cooling of the core through plate tectonics even without a superheated core and a transition to single-plate tectonics after about 500 Ma. [00Nim, 01Ste].

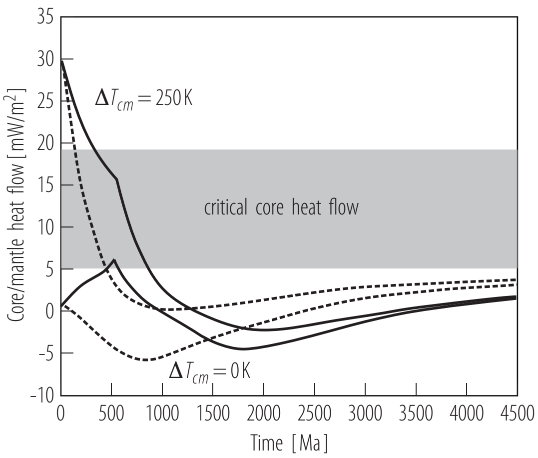

Fig. 3. Core-mantle heat flow as a function of time for models with early plate tectonics (solid line) and models with stagnant lid convection throughout the entire evolution (dashed line) with initial temperature differences across the core/mantle boundary of $\Delta T_{cm} = 0$ and $\Delta T_{cm} = 250$ K [after 03Bre]. The generation of a thermal dynamo is possible when the heat flow is larger than the critical core heat flow.

4.2.3.4.5.4 Moon

The thermal evolution of the Moon has remained a controversial subject. Early models start the evolution of the Moon with an accretionary initial temperature profile. This temperature profile increases from a relatively cold deep interior (less than 1000 K) to reach a maximum in the upper mantle from where temperature decreases towards the surface [86Mat]. Similar temperature profiles have been used in other models of the Moon's thermal evolution [73Cas, 78Tok, 79Cas].

More recent evolution models assume an initially hot interior [e.g., 77Sol, 78Min, 01Spo] but still open are questions about the thermal and structural state of the Moon after freezing of the magma ocean and whether convection is an important form of heat transport in the lunar interior. It is generally accepted that the anorthositc crust of the Moon formed as a floating crust on a magma ocean. Estimates of the depth of the primordial magmasphere, however, range from the whole Moon melting to thin melt layers above partially molten zones. Assuming that the magma ocean freezes rapidly during about 100 to 200 Ma [77Sol, 78Min] without any disturbances, this part of the mantle most likely became chemically stratified following magma ocean differentiation and crystallization with the late dense iron-rich phases coming to rest upon a less dense Mg-rich phase. Such a layering has strong implications for the subsequent evolution of the Moon since it is prone to convective overturn and mixing [95Hes, 98All]. It has also been speculated that during most of the Moon's history (i.e., after the first rapid overturn) heat might be transported by conduction alone [89Kir, 99Pri, 00Wie] as a consequence of the strong depletion of radioactive elements and stable chemical layering in the mantle.

Paleomagnetic data, combined with radiometric ages of Apollo samples, suggests that a field of possibly 1 G existed 4.0 Ga ago decreasing to a few thousand gamma 3.2 Ga ago [75Ste, 86Cis]. Because the present magnetic field of the Moon is negligible, [75Run] has argued that the lunar rocks were magnetized at the time of their origin by a field of internal origin. The easiest explanation for such a field is the operation of a dynamo in an iron-rich lunar core [e.g., 97Kon, 01Spo2, 03Ste]. Some researchers doubt that an internal dynamo is required to explain the magnetization of the Moon, and favour an alternative idea; the observed magnetic signature is suggested to be generated in association with large impacts during Moon's early history [72Hid, 84Hoo, 91Hoo, 01Hoo].

The surface heat flow of the Moon was measured by the Heat Flow Experiment on *Apollo 15* and *17.* This experiment was also attempted on *Apollo 16,* but failed due to a broken cable connection.

The Heat Flow Experiment involved drilling two holes into the regolith to depths of 1.6 - 2.3 meters. The temperature was measured at several depths within the hole. The rate at which temperature increases with depth is a measure of the heat flowing from the Moon's interior. The drilling caused some heating within the hole, although the effects of this heating decayed with time. Also, temperatures in the upper part of the regolith vary as the amount of incident sunlight changes throughout the lunar day and night. By monitoring temperatures in the drill holes over a long period of time, these effects can be accounted for, allowing for a determination of the average heat flow rate at the landing site.

The results of these measurements indicate a heat flow of 21 milliwatts per square meter at the *Apollo 15* landing site and of 16 milliwatts per square meter at the *Apollo 17* landing site. The Moon's heat flux is 18 - 24% of the Earth's average heat flux of 87 milliwatts per square meter. The small value of the lunar heat flow was expected, given the Moon's small size and the observation that it has been nearly dead volcanically for the last 3 billion years. Because the heat flow was measured at only two locations, it is not known how representative these values are for the Moon as a whole. However, because both measurements were obtained near boundaries between mare and highland regions, it is thought that the measured heat flows are probably 10-20% higher than the average value for the entire Moon. A recent discussion of the Apollo heat flow measurements can be found in [06She, 06Wie].

Table 8. Measured heat flow at the landing sites of Apollo 15 and Apollo 17.

	Heat flow
Apollo 15	21 mW/m^2
Apollo 17	16 mW/m^2

4.2.3.4.6 References for 4.2.3.4

65Toz Tozer, D.C.: Geophys. J. Int. **9** (1965) 95.
67Tur Turchotte, D.L., Oxburgh, E.R.: J. Fluid Mech. **28** (1967) 29.
72Hid Hide, R.: The Moon **4** (1972) 39.
73Cas Cassen, P., Reynolds, R.T.: J. Geophys. Res. **78** (1973) 3203.
73Sch Schubert, G., et al.: Nature **242** (1973) 251.
74Sie Siegfried, R.W., Solomon, S.C.: Icarus **23** (1974) 192.
75Run Runcorn, S.K.: Nature **253** (1975) 701.
75Ste Stephenson, A., et al.: Lun. Sci. Conf. **6** (1975) 3049.

75Str Strom, R.G., et al.: J. Geophys. Res. **80** (1975) 2478.
76Cas Cassen, P., et al.: Icarus **28** (1976) 501.
76Sha Sharpe, H.N., Strangway, D. W.: Geophys. Res. Lett. **3** (1976) 285.
76Sol Solomon, S.C.: Icarus **28** (1976) 509.
77And Anders, E.: Phil. Trans. Roy. Soc. Lond. **A285** (1977) 23.
77Rin Ringwood, A. E.: Geochem. J. **11** (1977) 111.
77Sol Solomon, S.C.: Phys. Earth Planet. Int. **15** (1977) 135.
77Wae Wänke, H., et al.: Phil. Trans. Roy. Soc. Lond. **A285** (1977) 41.
78Min Minear, J.W., Fletcher, C.R.: Lunar Planet. Sci. Conf. **9** (1978) 263.
78Tok Tokzös, M.N., et al.: NASA SP-370, (1978) 245.
78Wei Weidenschilling, S.J.: Icarus **35** (1978) 99.
79Cas Cassen, P., et al.: Phys. Earth Planet. Int. **19** (1979) 183.
79Kve Kvergvold, O.: Geophys. Astrophys. Fluid Dyn. **12** (1979) 273.
79Mor Morgan, J.W., Anders, E. Geochim. Cosmochim. Acta **43** (1979) 1601.
79Rob Roberts, G.O.: Geophys. Astrophys. Fluid Dyn. **12** (1979) 235.
79Sol Solomon, S.C.: Phys. Earth Planet. Int. **19** (1979) 168.
79Toz Tozer, D.C.: Phys. Earth Planet. Int. **18** (1979) 247.
79Wis Wise, D.U., et al.: J. Geophys. Res. **84** (1979) 7934.
80Mor Moroz, V.I., et al.: Nature **284** (1980) 243.
82Jar Jarvis, G.T., Peltier, W.R.: Geophys. J. R. Astron. Soc. **68** (1982) 389.
82Tay Taylor, S.R.: Phys. Earth Planet. Interiors **29** (1982) 233.
83Fri Frick, H., et al.: J. Fluid Mech. **127** (1983) 141.
83Mcc McCammon, C.A., et al.: Geophys. J. R. Astron. Soc. **72** (1983) 577.
83Ste Stevenson, D.J., et al.: Icarus **54** (1983) 466.
84Chr Christensen, U.R.: Phys. Earth Planet. Int. **35** (1984) 264.
84Hoo Hood, L.L., Vickery, A.: J. Geophys. Res. **89** (1984) C211.
84Wil Wilhelms, D.E., Squyres, S.W.: Nature **309** (1984) 138.
85Tay Taylor, S.R., McLennan, S.M.: The continental crust: Its origin and evolution, Blackwell Sci. Publ. Oxford, 1985.
85Sch Schubert, G., Anderson, C.A.: Geophys. J. R. astr. Soc. **80** (1985) 575.
86Cis Cisowski, S.M., Fuller, M.: Origin of the Moon, Lunar and Planetary Institute (1986) 411.
86Mat Matsui, T., Abe, Y.: Origin of the Moon, Lunar and Planetary Institute (1986) 453.
87Feg Fegley, B., Cameron, A.G.W.: Earth Planet. Sci. Lett. **82** (1987) 207.
86Tre Treiman, A.H., et al.: Geochim. Cosmochim. Acta **50** (1986) 1071.
88Cam Cameron, A.G., et al.: In: Vilas, F., et al., editors, Mercury, Univ. of Arizona Press, Tucson 692-708, 1988.
88Fre Frey, H., Schultz, R.A.: Geophys. Res. Lett. **15** (1988) 229.
88Sch Schubert, G., et al.: In: Vilas, F., et al., editors, Mercury, Univ. of Arizona Press, Tucson 514-561, 1988.
88Wet Wetherill, G.W.: In: Vilas, F., et al., editors, Mercury, Univ. of Arizona Press, Tucson 670-691, 1988.
89Kir Kirk, R.L., Stevenson, D.J.: J. Geophys. Res. **94 (B9)** (1989) 12133.
90Mcg McGill, G.E., Dimitriou, A.M.: J. Geophys. Res. **95** (1990) 12595.
90Sch Schubert, G., Spohn, T.: J. Geophys. Res. **95** (1990) 14095.
91Hoo Hood, L.L., Huang, Z.: J. Geophys. Res. **96** (1991) 9837.
91Rin Ringwood, A.E.: Geochim. Cosmochim. Acta **55** (1991) 2083.
91Spo Spohn, T.: Icarus **90** (1991) 222.
92Sch Schubert, G., et al.: In: Kieffer, H.H. et al., editors, Mars, Univ. of Arizona Press, Tucson 147-183, 1992.
93Bre Breuer, D., et al.: Planet. Space Sci. **41** (1993) 269.
93Han Hansen, U., Yuen, D.A.: Geophys. Res. Lett. **20** (1993) 2191.
93Kar Kargel, J.S., Lewis, J.S.: Icarus **105** (1993) 1.
93Pol Pollack, H.N., et al.: Rev. Geophys. **31** (1993) 267.
94Sle Sleep, N.H.: J. Geophys. Res. **99** (1994) 5639.

94Wae Wänke, H., et al.: Phil. Trans. R. Soc. Lond **A349** (1994) 285.
95Hes Hess, P.C., Parmentier, E.M.: Earth Planet. Sci. Lett. **134** (1995) 501.
95Mcd McDonough, W., Sun, S.S.: Chem. Geol. **120** (1995) 223.
95Mor Moresi, L.-N., Solomatov, V.S.: Phys. Fluid **7** (1995) 2154.
95Wei Weinstein, S.A.: J. Geophys. Res. **100 (E6)** (1995) 11719.
96Har Harder, H., Christensen, U.: Nature **380** (1996) 507.
96Sol Solomatov, V.S., Moresi, L.-N.: J. Geophys. Res. **101** (1996) 4737.
97Bou Basilevsky, A.T., et al.: In: Bougher, S.W., et al., editors, Venus II, Univ. of Arizona Press, Tucson 1047-1084, 1997.
97Doi Doin, M.-P., et al.: J. Geophys. Res. **102** (1997) 2771.
97 Kar Karato, S., Rubie, D.: J. Geophys. Res **102** (1997) 20111.
97Kon Konrad, W., Spohn, T.: Advances in Space Research **19(10)** (1997) 1511.
97Lod Lodders, K., Fegley B.: Icarus **126** (1997) 373.
97Mck McKenzie, D., Nimmo, F.: Icarus **130** (1997) 198.
98Acu Acuña, M.H., et al.: Science **279** (1998) 1676.
98All Alley, K.M., Parmentier, E.M.: Physics of Earth and Planetary Interiors **108** (1998) 15.
98Bre Breuer, D., et al.: Geophys. Res. Lett. **25** (1998) 229.
98Gra Grasset, O., Parmentier, E.M.: J. Geophys. Res. **103** (1998) 18171.
98Nim Nimmo, F., McKenzie, D.: Annual Review of Earth and Planetary Sciences **26** (1998) 23.
98Res Reese, C.C., et al.: J. Geophys. Res. **103** (1998) 13643.
98Spo Spohn, T., et al.: Astron. Astrophys. Rev. **8** (1998) 181.
99Acu Acuña, M.H., et al.: Science **284** (1999) 790.
99Cam Cameron, A.G.: Annual Review of Astronomy and Astrophysics. **37** (1999) 1.
99Con Conzelmann, V.: PhD-Thesis, Westfälische Wihlems-Universität Münster (1999).
99Con2 Connerney, J.E.P., et al.: Science **284** (1999) 794.
99Dum Dumoulin, C., et al.: J. Geophys. Res. **104** (1999) 12759.
99Har Hartmann, W.K., et al.: Nature **397** (1999) 586.
99Pri Pritchard, M.E., Stevenson, D.J.: The Origin of the Earth and Moon, Univ. of Arizona Press 1999.
99Res Reese, C.C., et al.: Icarus **139** (1999) 67.
99Smi Smith, D.E., et al.: Science **284** (1999) 1495.
00Des Deschamps, F., Sotin, C.: Geophys. J. Int. **143** (2000) 204.
00Har Harder, H.: Geophys. Res. Lett. **27** (2000) 301.
00Nim Nimmo, F., Stevenson, D. : J. Geophys. Res. **105** (2000) 11969.
00Sol Solomatov, V.S., Moresi, L.-N.: J. Geophys. Res. **105** (2000) 21795.
00Wie Wieczorek, M.A., Phillips, R.J.: J. Geophys. Res. **105** (2000) 20417.
00Zub Zuber, M.T., et al.: Science **287** (2000) 1788.
01Acu Acuña, M.H., et al.: J. Geophys. Res. **106** (2001) 23403.
01Hes Hess, P.C., Parmentier, E.M.: J. Geophys. Res. **106** (2001) 28023.
01Hoo Hood, L.L., et al.: J. Geophys. Res. **106** (2001) 27825.
01Sch Schubert, G., et al.: Mantle Convection in the Earth and Planets, Cambridge Univ. Press, Cambridge 2001.
01Sol Solomatov, V.S.: Earth Planet. Sci. Lett. **191** (2001) 203.
01Spo Spohn, T., et al.: Space Science Reviews **96** (2001) 231.
01Spo2 Spohn, T., et al.: Icarus **149** (2001) 54.
01Ste Stevenson, D.J.: Nature **412** (2001) 214.
01Wei Weizman, A., et al.: Icarus **150** (2001) 195.
01Zho Zhong, S., Zuber, M.T.: Earth Planet. Sci. Lett. **189** (2001) 75.
02Ber Berman, D.C., Hartmann, W.K.: Icarus **159** (2002) 1.
02Fre Frey, H.V., et al.: Geophys. Res. Lett. **29** (2002) 22-1.
02Hau Hauck, S.A., Philipps, R.J.: J. Geophys. Res. **107** (2002) 5052.
02Ste Stevenson, D.J.: American Geophysical Union, Spring Meeting 2002, abstract #P21A-08, (2002).
03Bre Breuer, D., Spohn, T.: J. Geophys. Res. **108** (2003) 5072.

03Ste Stegman, D. R. et al.: Nature **421(6919)** (2003) 143.
04Hau Hauck, S.A., et al.: Earth Planet. Sci. Lett. **222** (2004) 713.
04Neu Neukum, G., et al.: Nature **432** (2004) 971.
04Wen Wenzel, M.J., et al.: Geophys. Res. Lett. **31** (2004) L04702.
04Wil Williams J.-P., Nimmo, F.: Geology **32** (2004) 97.
05Con Connerney, J.E.P., et al.: Proc. Nat. Academy of Science **102** (2005) 14970.
05Elk Elkins-Tanton, L.T. et al.: J. Geophys. Res. **110** (2005) E12S01.
05Nim Nimmo, F., Tanaka, K.: Annual Review of Earth and Planetary Sciences **33** (2005) 133.
05Res Reese, C.C., et al.: Phys. Planet. Int. **149** (2005) 361.
05Sol Solomon, S.C., et al.: Science **307** (2005) 1214.
06Bon Bond, T.M., Warner, M.R.: Lun. Planet. Sci. Conf. **37** (2006) 1957.
06Bre Breuer, D., Spohn, T.: Planet. Space Sci. **54** (2006) 153.
06Bus Buske, M.: PhD-Thesis, ISBN 3-936586-58-6, Copernicus GmbH (2006)
06Iva Ivanov, M.A., Head, J.W: Lun. Planet. Sci. Conf. **37** (2006) 1366.
06Sch Schumacher, S., Breuer, D.: J. Geophys. Res. **111** (2006) E02006.
06She Shearer C.K., et al.: Reviews in Mineralogy & Geochemistry **60** (2006) 265.
06Wie Wieczorek, M.A., et al.: Reviews in Mineralogy & Geochemistry **60** (2006) 221.
07Bre Breuer, D., Moore, W.B.: In G. Schubert and T. Spohn, editors, Treatise on Geophysics-Planets and Moons, Volume **10**, pages 299-348. Elsevier, Amsterdam, 2007.
07Bre2 Breuer, D., et al.: Space Science Reviews **132** (2007) 229.
07Jau Jaupart, C., et al.: In G. Schubert and D. Bercovici, editors, Treatise on Geophysics-Mantle dynamics, Volume **7,** pages 253-303. Elsevier, Amsterdam, 2007.
07Sch Schubert, G., et al.: Icarus **188 (2)** (2007) 345.
08And Andrews-Hanna, J.C., et al.: Nature **453** (2008) 1212.
08Mar Marinova, M.M., et al.: Nature **453** (2008) 1216.
08Nim Nimmo, F., et al.: Nature **453** (2008) 1220.